CHEMICAL ENGINEERING TRANSACTIONS Volume 17, 2009
Editor Sauro Pierucci

 ISBN 978-88-95608-01-3 ISSN 1974-9791
DOI: 10.3303/CET0917168

Effect of Supercritical Deposition Synthesis on the Dibenzothiophene Hydrodesulfurization Activity over CoMo/Al-HMS Nanocatalyst

M. Alibouri[a,b], S. M. Ghoreishi[b,*], H. R. Aghabozorg[a]

[a]Catalysis Research Center, Research Institute of Petroleum Industry, Tehran 18745-4163, Iran
[b]Department of Chemical Engineering, Isfahan University of Technology, Isfahan 84156-83111, Iran
[*]Corresponding author E-mail: ghoreshi@cc.iut.ac.ir

The effect of supercritical impregnation was investigated in the hydrodesulfurization (HDS) of dibenzothiophene (DBT) by the preparation of CoMo/Al-HMS nanocatalyst. The supercritical deposition of catalytic metal (Mo) and promoter (Co) on the Al-HMS support was carried out in the catalyst preparation. Methanol was used as a modifier due to the limitation in the precursor's dissolution in the supercritical carbon dioxide. The characterization of the support and two catalysts (CoMo/Al-HMS nanocatalyst and $CoMo/Al_2O_3$ commercial catalyst) was accomplished by adsorption–desorption of nitrogen, and Temperature Programmed Reduction (TPR). A major incentive of the newly developed catalyst by supercritical deposition was realized in the higher and more uniform dispersion of the catalytic metal and promoter on the support. Another important advantage of this impregnation method was demonstrated via TPR curves in the reduction of Co and Mo species at lower temperatures in contrast to commercial catalyst. Conversion and selectivity of HDS of DBT was used in the catalyst activity evaluation. The experimental data indicated higher conversion at higher temperature for the new catalyst with respect to the commercial catalyst. The increased overall selectivity of cyclohexylbenzene to biphenyl in the two competitive reaction pathways, hydrogenation versus hydrogenolysis, which resulted in lower hydrogen consumption, is another improvement in the hydrodesulfurization process using the new catalyst. A higher activation energy (E/R) was calculated for the new catalyst (8231 K) in comparison to the commercial catalyst (5834 K) by applying linear Arrhenius' law to the calculated reaction rate constants at different temperatures with the assumption of pseudo first order reaction rate.

1. Introduction

The conventional method for the preparation of Mo supported catalysts is the incipient wetness impregnation with an ammonium heptamolybdate solution. Recently, supported metal nanoparticles have attracted a great deal of interest and their unique properties are directly related to the specific particle morphology (size and shape), metal dispersion, concentration and the electronic properties of the metal within their host environment (Stakheev and Kustov, 1991). Nanoparticles with high surface area supported on different support materials are currently used extensively as catalysts for chemical transformations. The surface of the nanoparticles plays an important role in their catalytic properties (Marino, et al. 2005; Carmo, et al. 2005). There are several ways to

Please cite this article as: Alibouri M., Ghoreishi S.M. and Aghabozorg R., (2009), Effect of supercritical deposition synthesis on the dibenzothiophene hydrodesulfurization activity over como/al-hms nanocatalyst, Chemical Engineering Transactions, 17, 1005-1010
DOI: 10.3303/CET0917168

synthesize supported nanoparticles, including microemulsion using organic stabilizing agents (Yu, et al. 2003), impregnation, deposition–precipitation, co-precipitation (Claus, et al., 2000), sonochemical reduction (Okitsu, et al. 1999), chemical vapor impregnation (Miller, et al. 1997), and sol–gel (Maldonado-Hodar, et al. 2000]. The control over either particle dimensions, including the particle size and distribution, or metal concentration in the composites remains the major problems for these methods due to the high surface tension of the liquid solutions. In this work, the synthesis, characterization, and the catalytic activity of CoMo/Al-HMS nanocatalyst in the reaction of HDS of DBT was investigated. The catalysts were characterized by adsorption–desorption of nitrogen, atomic adsorption technique, and TPR.

2. Experimental

2.1. Catalyst preparation

In preparation of the catalyst two metal salts as the source of catalytic metal and promoter were used: molybdenum hexacarbonyl (Mo $(CO)_6$) and cobalt nitrate ($Co(NO_3)_2.6H_2O$). Due to the much better solubility and phase behavior of $Mo(CO)_6$ in SC-CO_2 in comparison to $(NH_4)_6Mo_7O_{24}$, thus in this study $Mo(CO)_6$ was chosen as the main source of molybdenum to provide active sites of the catalyst. As the source of catalyst promoter, $Co(NO_3)_2.6H_2O$ was used but because of its insolubility in SC-CO_2, 6 wt% methanol was utilized as an entrainer, which can enhance the solvation power of SC-CO_2 significantly. The experimental set-up used in the synthesis of the catalyst is shown in Figure 1.

2.2. Catalyst evaluation

All catalysts were evaluated in a laboratory scale fixed bed flow reactor shown in Figure 2. Two model hydrocarbon feeds were used in this study: (1) n-heptane (Merck) + dibenzothiophene (DBT, Aldrich), and (2) n-heptane + toluene (Aldrich) + DBT.

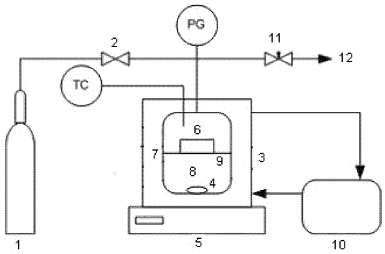

Figure 1: CO_2 cylinder, 2: valve, 3: bath, 4: magnetic stirrer, 5: stirrer, 6: basket, 7: vessel, 8: solution, 9: screen, 10: circulating heater and cooler, 11: needle valve, 12: vent

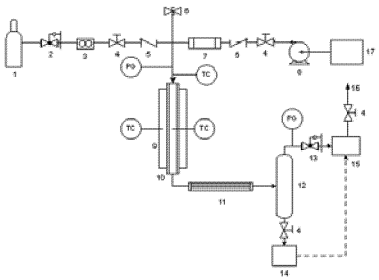

Figure 2: H_2 cylinder, 2: pressure reducer, 3: mass flow meter, 4: screw-down valve, 5: check valve, 6: relief valve, 7: evaporator, 8: pump, 9: furnace, 10: reactor, 11: condenser, 12: separator, 13: back pressure regulator, 14: liquid trap, 15: GC, 16: vent, 17: liquid feed, TC: thermocouple, PG: pressure gauge

The reaction scheme for DBT desulfurization has been proposed (Houalla, et al. 1980) in accordance with the hydrogenolysis pathway, through the direct desulfurization route

(DDS), leading to the production of biphenyl (BP), or by a second hydrogenation reaction pathway (HYD), in which one of the aromatic rings of dibenzothiophene is firstly prehydrogenated, forming tetrahydrodibenzothiophene and hexahydrodibenzothiophene, which is later desulfurized to form cyclohexylbenzene (CHB). For the synthesized and commercial catalysts, the main products of the reaction were BP and CHB in addition to unreacted DBT. Based on the conversion and selectivity data, assuming the pseudo first order with respect to DBT, and convective mass transfer mechanism (neglecting axial dispersion coefficient: $D_z \rightarrow 0$ or in other words, $N_{Pec} \rightarrow \infty$), the reaction rate constant of HDS (k_{HDS}) was calculated according to the one dimensional axial mass balance equation for the plug flow reactor:

$$k_{HDS} = -(F/W)\ln(1-x) \quad (1)$$

$$k_{HDS} = k_0 \exp(-E/RT) \quad (2)$$

in which F is the feed rate of DBT (mol/min), W is the catalyst weight (g), x is the mole fractional conversion of DBT, k_0 is the frequency factor (mol/g cat. min) and E is the activation energy (K). Hydrogenolysis (DDS) and hydrogenation (HYD) overall selectivity was calculated according to the formula (C_i =component concentration):

$$S_o = C_{CHB}/C_{BP} \quad (3)$$

3. Results and discussion

3.1. Catalyst characterization

The physical adsorption-desorption of nitrogen was used to determine the textural properties of Al-HMS support and CoMo/Al-HMS nanocatalyst. The obtained results are shown in Figure 3. At low relative pressure, the N_2 uptake increases sharply as the N_2 pressure increase, which indicates that the support has a very high surface area. In addition, there is another sharp increase in the range of P/P_0 = 0.2–0.3 in the isotherms. This sharp increase in uptake results from the capillary condensation of N_2, which suggests that uniform mesopores are present in the Al-HMS. All the isotherms are type-IV shapes and the uptake of N_2 decreases with the loading of the metal species on the support. Figure 4 shows the pore size distributions of the support and catalyst. It should be noted from Figure 4 that the pore size distribution curves are for two different cases; the first one is for the Al-HMS support with a median pore diameter of 26 ^{o}A and the second for the support with loaded Co and Mo oxide with a pore diameter of 24.8 ^{o}A.

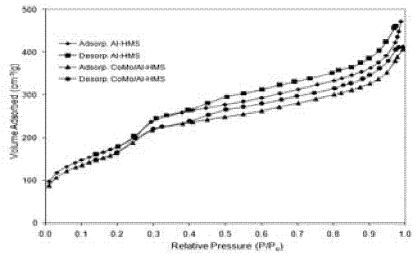

Figure 3. N_2 adsorption–desorption isotherms of Al-HMS and CoMo/Al-HMS

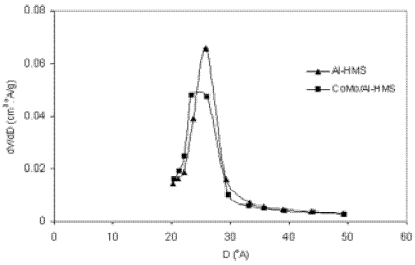

Figure 4. Pore size distribution of Al-HMS and CoMo/Al-HMS

The uniform and narrow pore size distributions of the support and catalyst provide independent verification of retention of pore structure after impregnation of the metal oxide precursors. There appears to be a pore diameter shift to smaller diameter upon of supercritical deposition of Co and Mo on the Al-HMS support. Therefore, the results in Figure 4 indicates a major advantage of using supercritical deposition in which no pore plugging occurs and it further reveals that the internal surfaces of Al-HMS pores is even though slightly reduced but its textural characteristics does not change.

The TPR curves of the catalyst in the oxide form and of bulk Co_2O_3 and MoO_3 are shown in Figure 5. It is well established that the peaks shift to lower temperature when the support is proton-exchanged and the peaks shift to higher temperature when the Al is added to the support (Al-HMS). Comparison of the TPR pattern in this study with commercial catalyst and other TPR profiles in literature (Zepeda, et al. 2006) indicates that the reduction of Co and Mo species in the supported catalyst synthesized via supercritical deposition occurs at lower temperatures. The observed higher intensity peaks of the synthesized nanocatalyst with respect to commercial catalyst are obviously indicative of higher consumption of hydrogen in the TPR curves for the newly developed catalyst.

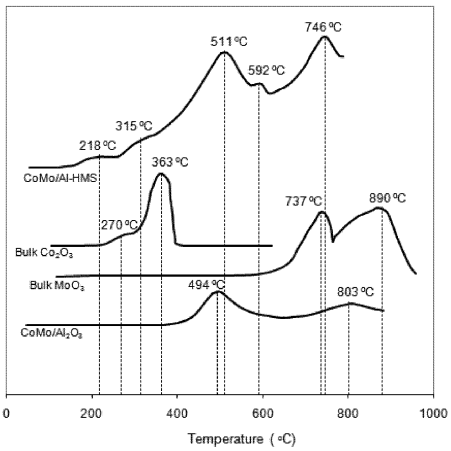

Figure 5. TPR curves of the catalysts and of bulk Co_2O_3 and MoO

3.2. Catalyst activity

In the present study, the catalytic performance of sulfided CoMo/Al-HMS nanocatalyst in terms of conversion and selectivity was examined in the HDS of DBT; DBT was chosen as the hydrocarbon model compound because it is one of the most refractory sulfur compounds in gas oil. For comparison purposes, commercial CoMo catalyst supported on alumina ($CoMo/Al_2O_3$) was also evaluated in the HDS of DBT.

Figure 6 shows the conversion of DBT in the HDS using synthesized CoMo/Al-HMS nanocatalyst and commercial catalyst as a function of temperature. The synthesized CoMo/Al-HMS nanocatalyst shows higher conversion of DBT into BP and CHB at higher temperatures. For instance, conversion of 61.2% was obtained using CoMo/Al-HMS nanocatalyst at 320 ^oC in contrast to 51.0% for the commercial catalyst. This enhanced conversion may be explained in terms of exponential temperature effect

on the reaction rate constant using the catalyst with higher activation energy according to the Arrhenius' law. As the supporting evidence for this phenomenon the calculated reaction rate constants of HDS at temperatures of 260 °C to 320 °C are summarized in Table 1. The reaction rate constant for the CoMo/Al-HMS nanocatalyst at 320 °C increased about 32.4% with respect to the conventional catalyst. As shown in Table 2, the activation energy and frequency factor for the synthesized and commercial catalyst was calculated according to the Arrhenius' law. As mentioned above, the activation energy of the synthesized catalyst is much higher (about 41%) than the commercial catalyst which, is the indication another major incentive for the new the developed catalyst in this study. In other words, higher obtained activation energy provides improved catalyst performance at lower temperature. Figure 7 shows the effect of new catalyst on the selectivity of CHB over BP. For all temperatures, higher selectivity is obtained for the newly developed nanocatalyst with respect to the commercial catalyst.

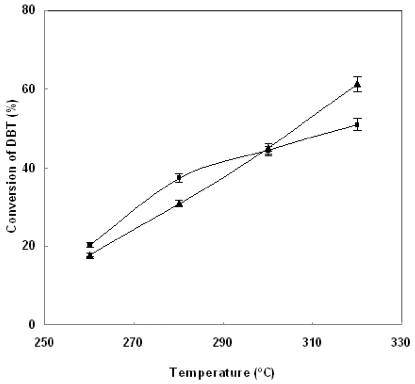

Figure 6. Conversion of DBT as a function of temperature (▲) CoMo/Al-HMS, (■)CoMo/Al_2O_3

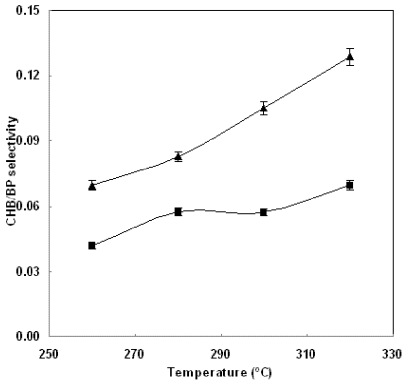

Figure 7. Variation of CHB/BP selectivity (▲) CoMo/Al-HMS, (■) CoMo/Al_2O_3

Table 1. Reaction rate constants for HDS of DBT (mol /g cat. min10^5)*

Catalyst	260 °C	280 °C	300 °C	320 °C
CoMo/Al-HMS	0.50	0.94	1.51	2.41
CoMo/Al_2O_3	0.58	1.19	1.49	1.82

Table 2. Activation energy and frequency factor for the synthesized CoMo/Al-HMS nanocatalyst and CoMo/Al_2O_3 commercial catalyst

Catalyst	k_0 (mol /g cat. min)	E/R (K)
CoMo/Al-HMS	2.60 * 10^6	8231
CoMo/Al_2O_3	3.74 * 10^4	5834

4. Conclusion

The supercritical CO_2–methanol impregnation of metal salts in the synthesis of CoMo/Al-HMS improved the catalytic activity in the hydrodesulfurization of DBT in comparison to the commercial catalyst. Higher metal dispersion and uniformity on the Al-HMS support, reduced particle size, increased active sites, higher activation energy, reaction rate constant, and conversion is the direct result of the special properties of supercritical fluid (high diffusivity and density, low viscosity and surface tension) in the deposition of metals on the support.

Acknowledgment

The financial support provided by National Iranian Oil Company (NIOC) and Isfahan University of Technology (IUT) is gratefully acknowledged.

References

Carmo, M., Paganin, V.A., Rosolen, J.M., and Gonzalez, E.R., 2005, Alternative supports for the preparation of catalysts for low-temperature fuel cells: the use of carbon nanotubes, J. Power Sources 142, 169-176.

Claus, P., Bruckner, A., Mohr, C., and Hofmeister, H., 2000, Supported gold nanoparticles from quantum dot to mesoscopic size scale: effect of electronic and structural properties on catalytic hydrogenation of conjugated functional groups, J. Am. Chem. Soc. 122, 11430-11439.

Houalla, M., Broderick, D.H., Sapre, A.V., Naga, N.K.,. de Beer, V.H.J, Gates, B.C., and Kwart, H., 1980, Hydrodesulfurization of methyl-substituted dibenzothiophenes catalyzed by sulfided CoMo/γ-Al2O3, J. Catal. 61, 523-527.

Maldonado-Hodar, F.J., Moreno-Castilla, C., Rivera-Utrilla, J., and Ferro Garcia, M.A., 2000, Metal-carbon aerogels as catalysts and catalyst supports, Stud. Surf. Sci. Catal. 130, 1007-1013.

Marino, F., Descorme, C., and Duprez, D., 2005, Supported base metal catalysts for the preferential oxidation of carbon monoxide in the presence of excess hydrogen (PROX), Appl. Catal. B: Environ. 58, 175-183.

Miller, J.M., Dunn, B., Tran, T.D., and Pekala, R.W., 1997, Deposition of ruthenium nanoparticles on carbon aerogels for high energy density supercapacitor electrodes, J. Electrochem. Soc. 144, 309-311.

Okitsu, K., Nagaoka, S., Tanabe, S., Matsumoto, H., Mizukoshi, Y., Nagata, Y., 1999, Sonochemical preparation of size-controlled palladium nanoparticles on alumina surface, Chem. Lett. 3, 271-272.

Stakheev, A.Y., and Kustov, L.M. 1999, Effects of the support on the morphology and electronic properties of supported metal clusters: modern concepts and progress in 1990s, Appl. Catal. A 188, 3-35.

Yu, K.M.K., Yeung, C.M.Y., Thompsett, D., and Tsang, S.C., 2003, Aerogel-coated metal nanoparticle volloids as novel entities for the synthesis of defined supported metal catalysts, J. Phys. Chem. B 107, 4515-4526.

Zepeda, T.A., Halachev, T., Pawelec, B., Nava, R., Klimova, T., Fuentes, G.A., and Fierro, J.L.G. 2006, Hydrodesulfurization of dibenzothiophene over CoMo/HMS and CoMo/Ti-HMS catalysts, Cata. Commun. 7, 33–41.